Tables and table legends.

Table 1 (related to Figure 1). Data for primary screen of FDA-approved drugs in HuH-7 cells. Plate number and location, product number and drug name, percent infection are provided as well as percent infection and cell numbers are provided for both replicates. Z score for each percent infection is provided. Table is provided as excel file.

Table S2 (see also Table 2)

Drug	**Target Gene**	**siRNA YFV hits**	**Relationship**
Palonosetron-HCL	HTR3A	HTR3C	Subunits of the serotonin receptor 5-HT3.
Digoxin	ATP1A1	ATP1B1	Subunits of the Na+/K+ ATPase (also known as the Na+/K+ pump).
Fingolimod	Sphingosine-1—phosphate receptor 1	EDG1	Sphingosine-1—phosphate receptor 1
Drug	**Target Gene**	**siRNA DENV hits**	**Relationship**
Bortezomib	Proteasome	PSMB6 PSMD2	Subunits of the proteasome

Table 2 (related to Table 2) Pathways in common between RNAi-based screens and drug screen.

Figure S1

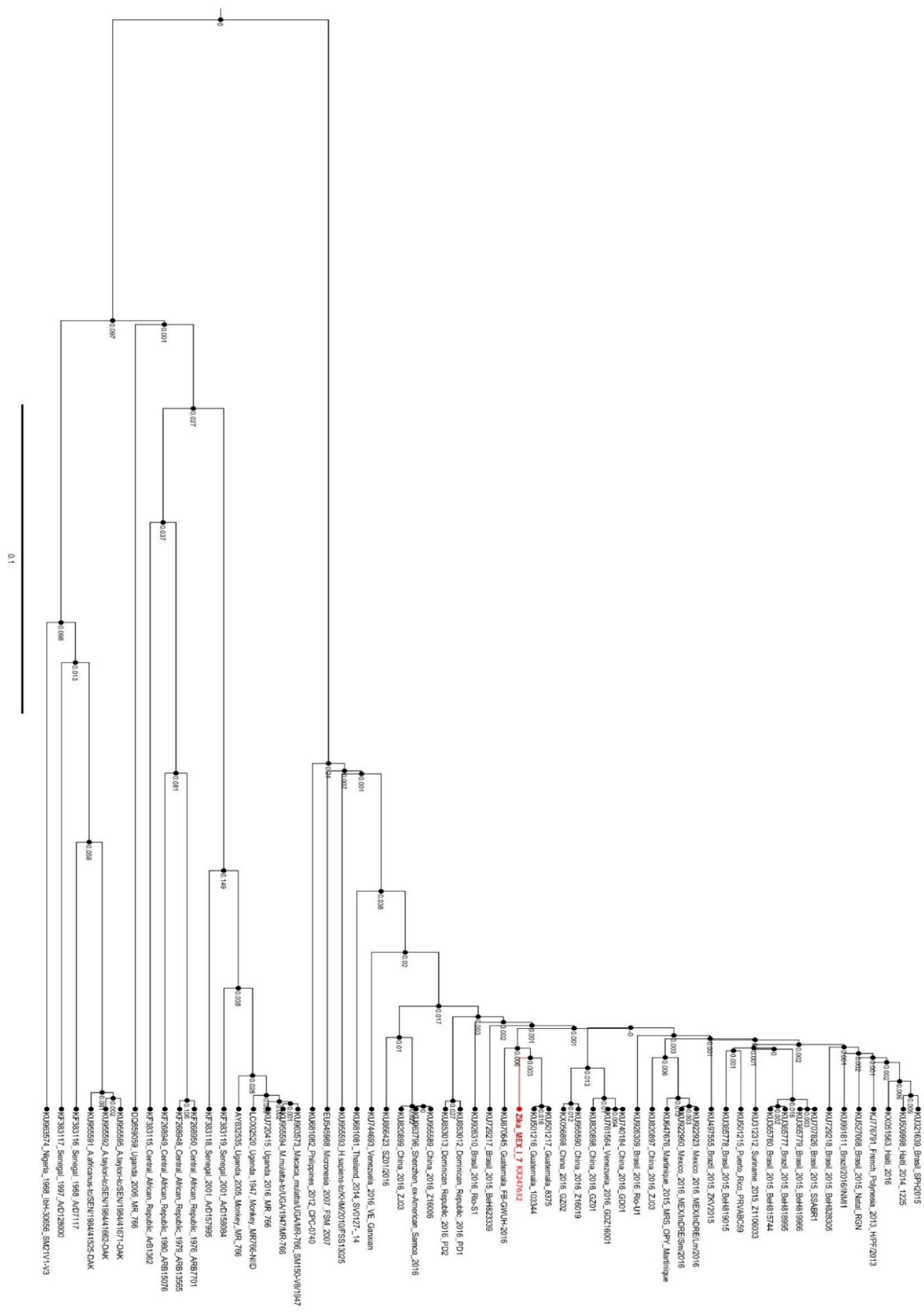

Figure S2

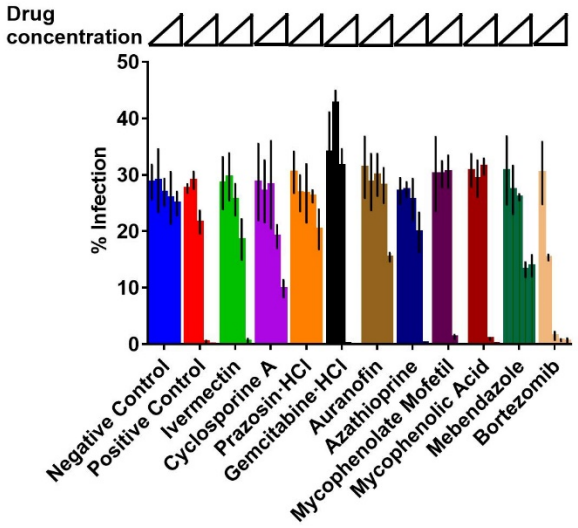
Drug concentration
% Infection
50
40
30
20
10
0
Negative Control
Positive Control
Ivermectin
Cyclosporine A
Prazosin·HCl
Gemcitabine·HCl
Auranofin
Azathioprine
Mycophenolate Mofetil
Mycophenolic Acid
Mebendazole
Bortezomib

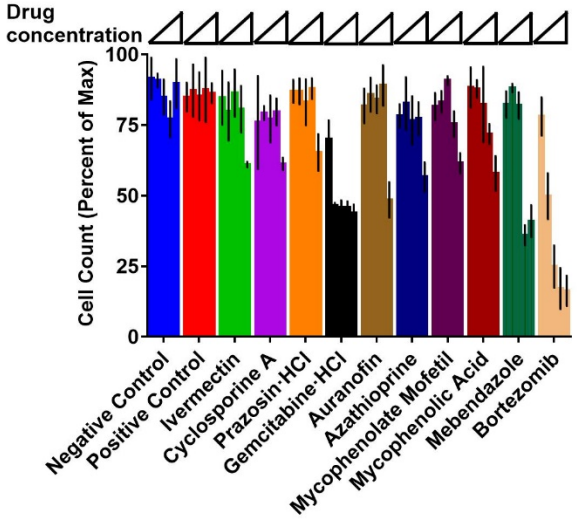
Drug concentration
Cell Count (Percent of Max)
100
75
50
25
0
Negative Control
Positive Control
Ivermectin
Cyclosporine A
Prazosin·HCl
Gemcitabine·HCl
Auranofin
Azathioprine
Mycophenolate Mofetil
Mycophenolic Acid
Mebendazole
Bortezomib

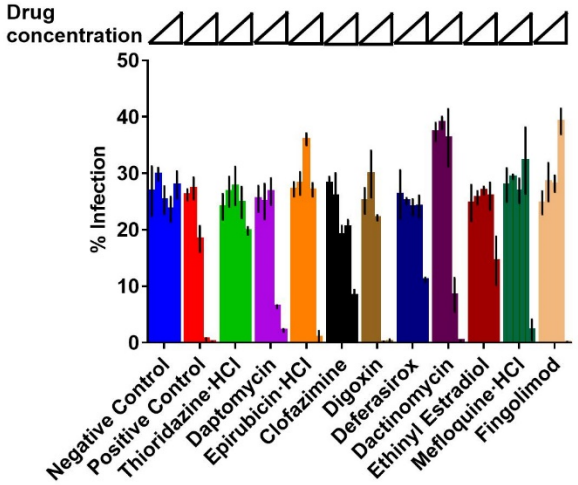
Drug concentration
% Infection
50
40
30
20
10
0
Negative Control
Positive Control
Thioridazine·HCl
Daptomycin
Epirubicin·HCl
Clofazimine
Digoxin
Deferasirox
Dactinomycin
Ethinyl Estradiol
Mefloquine·HCl
Fingolimod

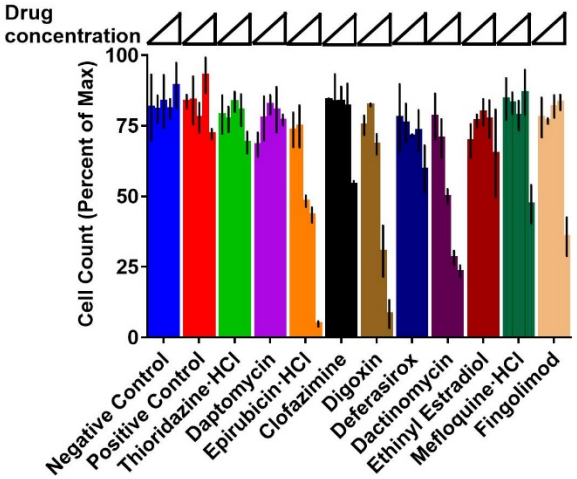
Drug concentration
Cell Count (Percent of Max)
100
75
50
25
0
Negative Control
Positive Control
Thioridazine·HCl
Daptomycin
Epirubicin·HCl
Clofazimine
Digoxin
Deferasirox
Dactinomycin
Ethinyl Estradiol
Mefloquine·HCl
Fingolimod

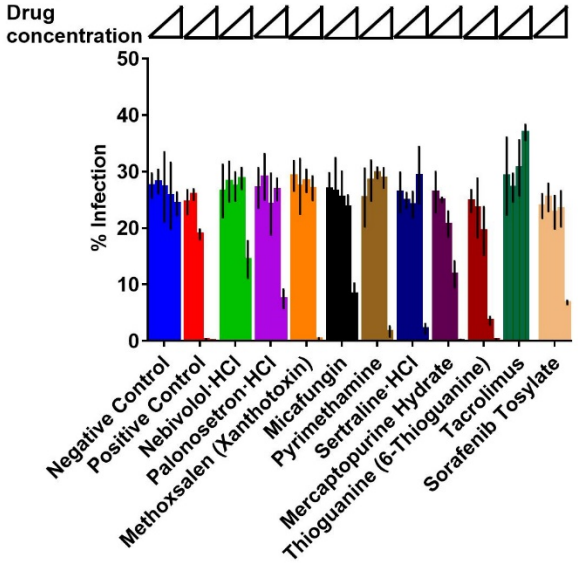
Drug concentration
% Infection
50
40
30
20
10
0
Negative Control
Positive Control
Nebivolol·HCl
Palonosetron·HCl
Methoxsalen (Xanthotoxin)
Micafungin
Pyrimethamine
Sertraline·HCl
Mercaptopurine Hydrate
Thioguanine (6-Thioguanine)
Tacrolimus
Sorafenib Tosylate

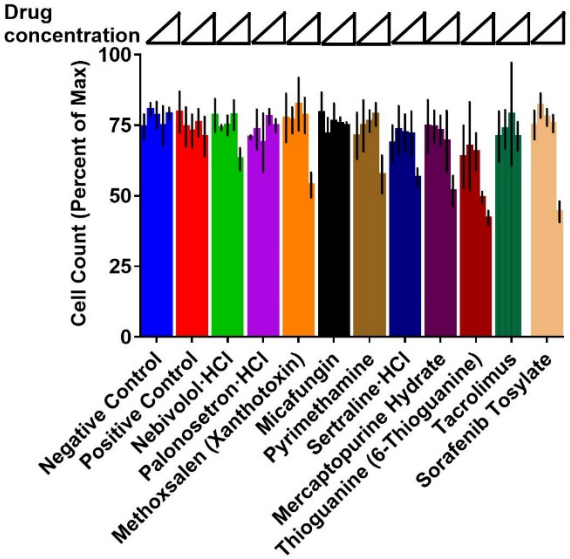
Drug concentration
Cell Count (Percent of Max)
100
75
50
25
0
Negative Control
Positive Control
Nebivolol·HCl
Palonosetron·HCl
Methoxsalen (Xanthotoxin)
Micafungin
Pyrimethamine
Sertraline·HCl
Mercaptopurine Hydrate
Thioguanine (6-Thioguanine)
Tacrolimus
Sorafenib Tosylate

Figure S3

A

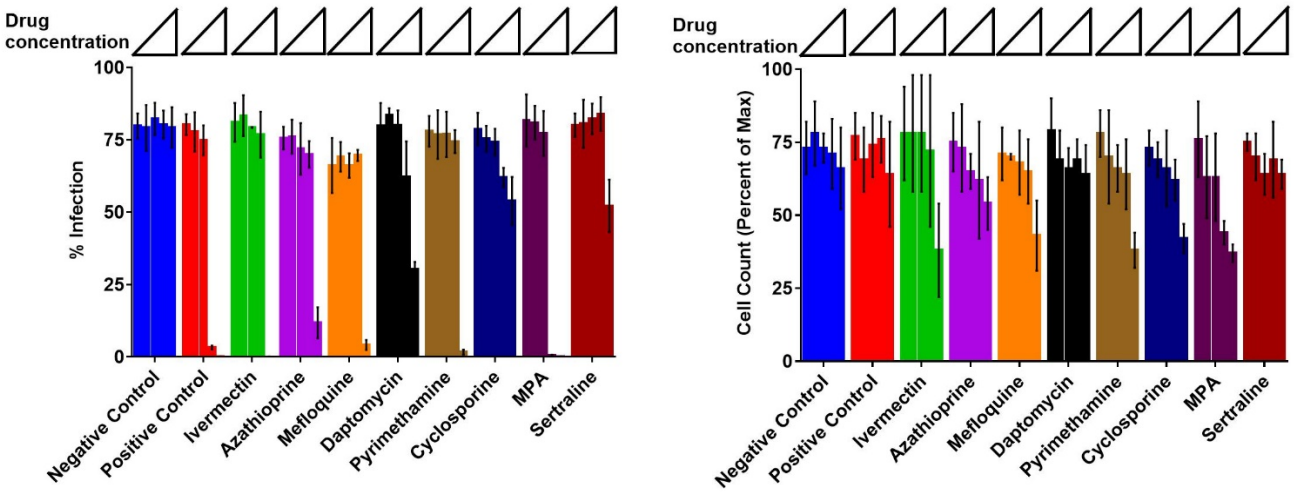
Drug concentration
% Infection
Cell Count (Percent of Max)
100
75
50
25
0
Negative Control
Positive Control
Ivermectin
Azathioprine
Mefloquine
Daptomycin
Pyrimethamine
Cyclosporine
MPA
Sertraline

B

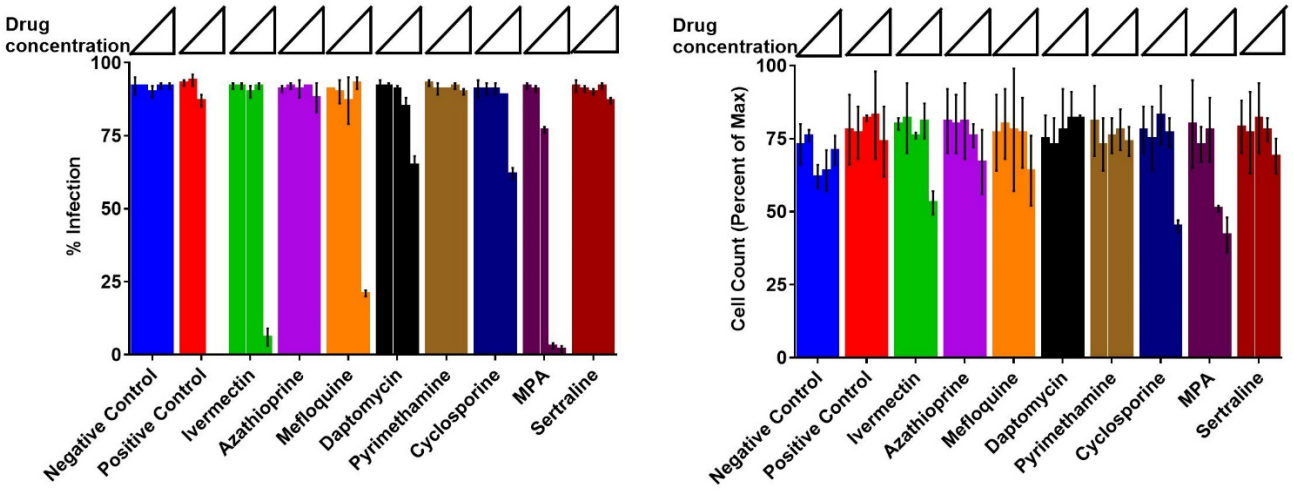
Drug concentration
% Infection
Cell Count (Percent of Max)
100
75
50
25
0
Negative Control
Positive Control
Ivermectin
Azathioprine
Mefloquine
Daptomycin
Pyrimethamine
Cyclosporine
MPA
Sertraline

Figure S4

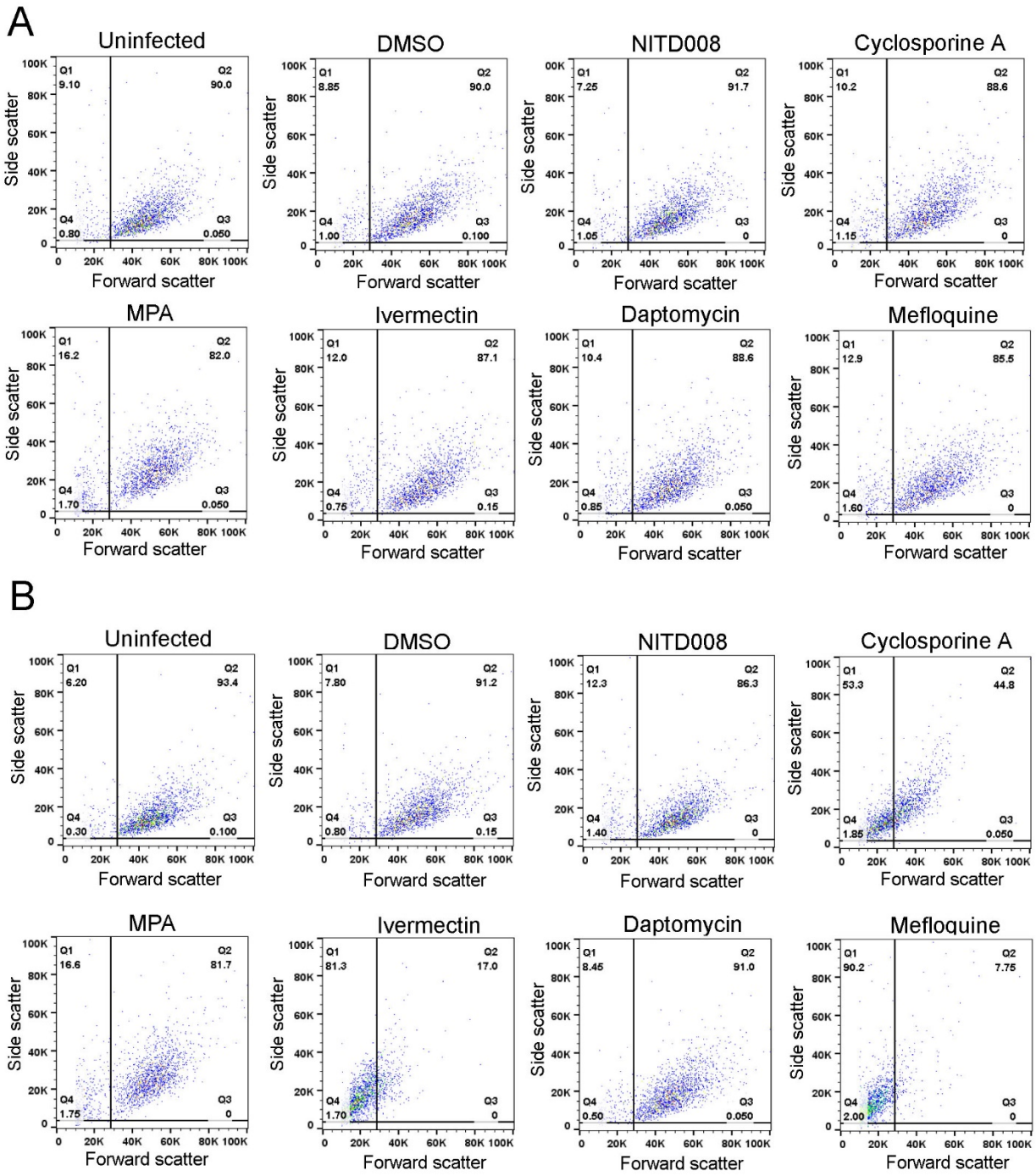
A
Uninfected
Q1 9.10
Q2 90.0
Q4 0.80
Q3 0.050
DMSO
Q1 8.85
Q2 90.0
Q4 1.00
Q3 0.100
NITD008
Q1 7.25
Q2 91.7
Q4 1.05
Q3 0
Cyclosporine A
Q1 10.2
Q2 88.6
Q4 1.15
Q3 0
MPA
Q1 16.2
Q2 82.0
Q4 1.70
Q3 0.050
Ivermectin
Q1 12.0
Q2 87.1
Q4 0.75
Q3 0.15
Daptomycin
Q1 10.4
Q2 88.6
Q4 0.85
Q3 0.050
Mefloquine
Q1 12.9
Q2 85.5
Q4 1.60
Q3 0
B
Uninfected
Q1 6.20
Q2 93.4
Q4 0.30
Q3 0.100
DMSO
Q1 7.80
Q2 91.2
Q4 0.80
Q3 0.15
NITD008
Q1 12.3
Q2 86.3
Q4 1.40
Q3 0
Cyclosporine A
Q1 53.3
Q2 44.8
Q4 1.85
Q3 0.050
MPA
Q1 16.6
Q2 81.7
Q4 1.75
Q3 0
Ivermectin
Q1 81.3
Q2 17.0
Q4 1.70
Q3 0
Daptomycin
Q1 8.45
Q2 91.0
Q4 0.50
Q3 0.050
Mefloquine
Q1 90.2
Q2 7.75
Q4 2.00
Q3 0
Side scatter
Forward scatter
0 20K 40K 60K 80K 100K

Supplementary Figure S5

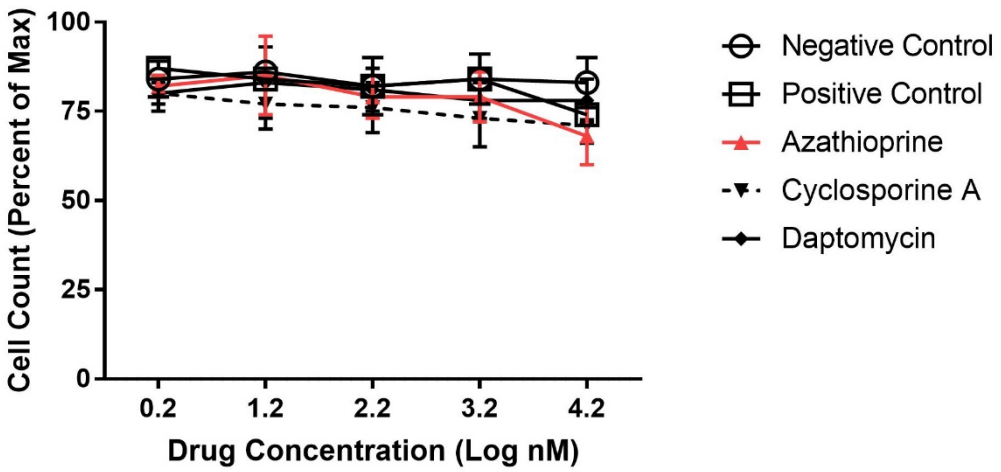

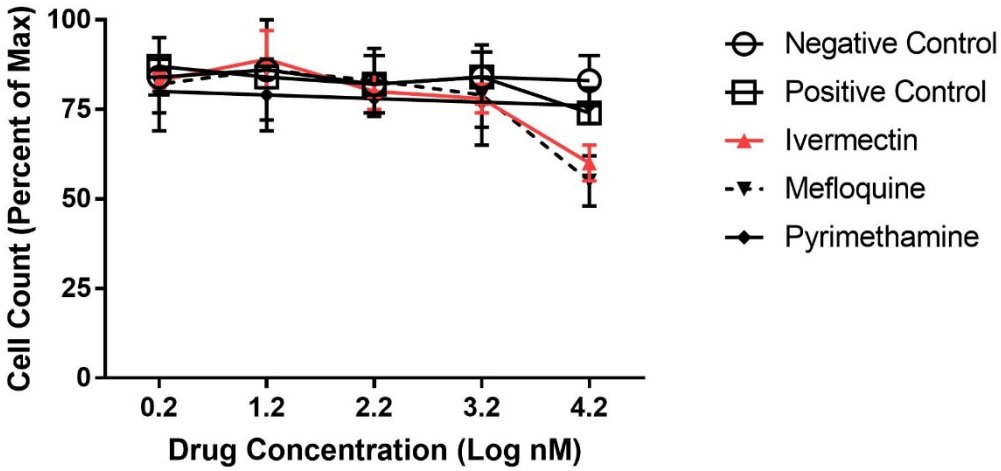

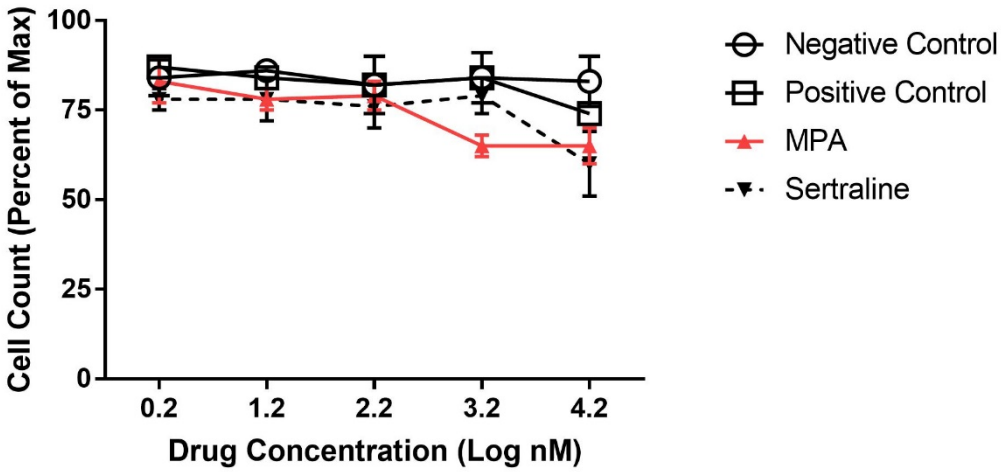

Supplementary Figure Legends

Figure S1 (Related to Figure 1)**.** Phylogenetic analysis of the ZIKV MEX_I_7 (GenBank KX247632) isolate (red) shows similarity to other American epidemic strains.

Figure S2 (Related to Figure 2)**.** Validation data for 30 selected drugs in HuH-7 cells. Infection rates (left panels) and cells counts (right panels) are shown for each drug tested alongside positive and negative control data. Drug concentrations (triangle) for each drug increase left to right at 0.001, 0.01, 0.1, 1.0 and 10 μM concentrations and then infections were performed as detailed in Experimental Procedures. Data are represented as mean +/- standard deviation.

Figure S3 (Related to Figure 3). Validation of selected drugs on HeLa cells (A) and JEG3 cells (B). Infection rates (left panels) and cells counts (right panels) are shown for each drug tested alongside positive and negative control data. Drug concentrations (triangle) for each drug increase left to right from 0.001μM to 10μM similar to Figure S2. Data are represented as mean +/- standard deviation.

Figure S4 (Related to Figure 4)**.** Flow cytometry data of ZIKV-infected hNSCs. (A) Effects of indicated drugs at 1 μM concentration on light scattering are shown. The population of cells in the upper right quadrants of scatter diagrams were analyzed for infection rate. (B) Same as in (A) except drug concentrations equal 10 μM.

Figure S5 (Related to Figure 5)**.** Cell count (percent of maximum) data for the HAECs tested for ZIKV infection after drug treatment relative to drug concentration. Each drug was used to treat cells at 0.0016, 0.016, 0.16, 1.6 and 16 μM concentrations and then infections were performed as detailed in Experimental Procedures. Cells counts are shown for each drug tested alongside positive (NITD008) and negative (DMSO) control data. The corresponding infection rates is shown in Figure 5. Data are represented as mean +/- standard deviation

Supplementary Experimental Procedures.

ZIKV/MEX_I_7/2015 resequencing and phylogeny. Next-generation sequencing libraries were generated from purified ZIKV genomic RNA using 'ClickSeq' Azido-terminated cDNA method (Routh et al., 2015b). Purified libraries and size selected libraries were sequenced on an Illumina MiSeq using v3 chemistry for 1 x 301 cycles and 7 indexing cycles. Sequences were demultiplexed using the MiSeq Reporter Software (MSR).

Raw FASTQ data were quality filtered as described previously (Routh et al., 2015a), yielding 1.2M reads with 98% PHRED scores greater than 20. Reads were aligned end-to-end using bowtie2 to the ZIKV KU955595. Mismatched mapped nucleotides with PHRED score > 30 were counted using in house scripts and the original reference genome was corrected if variant nucleotides or InDels were present at a frequency > 50%. This alignment and reference correction process was iterated three times, when the number of reads successfully mapping to the reference genome did not increase. This corrected sequence for the ZIKV MEX_I_7 isolate is deposited in GenBank under accession number KX247632. Sequence coverage was greater than 100 for nucleotides: 3-10,770.

For phylogenetic analysis, in addition to our ZIKV MEX_1_7 isolate, all complete Zika virus genomes (65 in total) were obtained from NCBI and coding sequences were extracted using VIGOR (Wang et al., 2012) The nucleotide CDSs were aligned with MUSCLE using standard parameters via the EBI-EMBL MUSCLE server (McWilliam et al., 2013) and first iteration trees were illustrated using FigTree v1.4.2 (http://tree.bio.ed.ac.uk/software/figtree/).

Recently, Cheng and colleagues identified 34 amino acid changes that were uniquely shared by American ZIKV isolates, including ZIKV Rio-U1, and distinguished these viruses from the older Asian isolates, P6-740 and FSS13025 (Wang et al., 2016). After pairwise comparison between ZIKV P6-740, FSS13025, Rio-U1 and MEX_I_7, we determined that ZIKV MEX_I_7 shares all 34 amino acid changes with the recent isolate ZIKV Rio-U1, further establishing ZIKV MEX_I_7 as an American pandemic isolate.

Supplementary References

McWilliam, H., Li, W., Uludag, M., Squizzato, S., Park, Y.M., Buso, N., Cowley, A.P., and Lopez, R. (2013). Analysis Tool Web Services from the EMBL-EBI. Nucleic acids research *41*, W597-600.

Routh, A., Chang, M.W., Okulicz, J.F., Johnson, J.E., and Torbett, B.E. (2015a). CoVaMa: Co-Variation Mapper for disequilibrium analysis of mutant loci in viral populations using next-generation sequence data. Methods *91*, 40-47.

Routh, A., Head, S.R., Ordoukhanian, P., and Johnson, J.E. (2015b). ClickSeq: Fragmentation-Free Next-Generation Sequencing via Click Ligation of Adaptors to Stochastically Terminated 3'-Azido cDNAs. Journal of molecular biology *427*, 2610-2616.

Wang, L., Valderramos, S.G., Wu, A., Ouyang, S., Li, C., Brasil, P., Bonaldo, M., Coates, T., Nielsen-Saines, K., Jiang, T.*, et al.* (2016). From Mosquitos to Humans: Genetic Evolution of Zika Virus. Cell host & microbe *19*, 561-565.

Wang, S., Sundaram, J.P., and Stockwell, T.B. (2012). VIGOR extended to annotate genomes for additional 12 different viruses. Nucleic acids research *40*, W186-192.